

# Single spin asymmetries in $\ell p^\uparrow \rightarrow hX$ processes and transverse momentum dependent factorization

M. Anselmino,<sup>1,2</sup> M. Boglione,<sup>1,2</sup> U. D'Alesio,<sup>3,4,\*</sup> S. Melis,<sup>1</sup> F. Murgia,<sup>4</sup> and A. Prokudin<sup>5</sup>

<sup>1</sup>*Dipartimento di Fisica Teorica, Università di Torino, Via P. Giuria 1, I-10125 Torino, Italy*

<sup>2</sup>*INFN, Sezione di Torino, Via P. Giuria 1, I-10125 Torino, Italy*

<sup>3</sup>*Dipartimento di Fisica, Università di Cagliari, I-09042 Monserrato (CA), Italy*

<sup>4</sup>*INFN, Sezione di Cagliari, C.P. 170, I-09042 Monserrato (CA), Italy*

<sup>5</sup>*Jefferson Laboratory, 12000 Jefferson Avenue, Newport News, Virginia 23606, USA*

(Received 5 May 2014; published 30 June 2014)

Some estimates for the transverse single spin asymmetry,  $A_N$ , in the inclusive processes  $\ell p^\uparrow \rightarrow hX$ , given in a previous paper, are expanded and compared with new experimental data. The predictions are based on the Sivers distributions and the Collins fragmentation functions which fit the azimuthal asymmetries measured in semi-inclusive deep inelastic scattering (SIDIS) processes ( $\ell p^\uparrow \rightarrow \ell' hX$ ). The factorization in terms of transverse momentum dependent distribution and fragmentation functions (TMD factorization)—i.e. the theoretical framework in which SIDIS azimuthal asymmetries are analyzed—is assumed to hold also for the inclusive process  $\ell p \rightarrow hX$  at large  $P_T$ . The values of  $A_N$  thus obtained agree in sign and shape with the data. Some predictions are given for future experiments.

DOI: 10.1103/PhysRevD.89.114026

PACS numbers: 13.88.+e, 13.60.-r, 13.85.Ni

## I. INTRODUCTION

In a previous paper [1] the issue of the validity of the TMD factorization for hard inclusive processes in which only one large scale is detected has been investigated in a simple phenomenological approach. We considered transverse Single Spin Asymmetries (SSAs) for the  $\ell p^\uparrow \rightarrow hX$  process, with the detection, in the lepton-proton center of mass (c.m.) frame, of a single large  $P_T$  final particle, typically a pion. Also the case of jet production,  $\ell p^\uparrow \rightarrow \text{jet} + X$ , was considered. The final lepton is not necessarily observed; however, a large value of  $P_T$  implies, at leading perturbative order, large values of  $Q^2$ , and the active role of a hard elementary interaction,  $\ell q \rightarrow \ell' q$ . Such a measurement is the exact analogue of the SSAs observed in the  $pp^\uparrow \rightarrow hX$  processes, the well known and large left-right asymmetries  $A_N$ , measured over a huge energy range [2–12]. On the other hand, the process is essentially a semi-inclusive deep inelastic scattering (SIDIS) process, for which, at large  $Q^2$  values (and small  $P_T$  in the  $\gamma^* - p$  c.m. frame), the TMD factorization is proven to hold [13–20].

We computed these SSAs assuming the TMD factorization and using the relevant TMDs (Sivers and Collins functions) as extracted from SIDIS data. A similar idea of computing left-right asymmetries in SIDIS processes, although with different motivations and still demanding the observation of the final lepton, has been discussed in Ref. [21]. A first simplified study of  $A_N$  in  $\ell p^\uparrow \rightarrow hX$  processes was performed in Ref. [22]. The process was also considered in Refs. [23,24] in the framework of collinear

factorization with twist-three correlation functions, obtaining asymmetries with a sign opposite to that of the corresponding ones in  $pp$  processes. Jet production in  $\ell p \rightarrow \text{jet} + X$  was studied in Ref. [25], in a collinear factorization scheme with a higher-twist quark-gluon-quark correlator,  $T_F$ , which is related to the first moment of the Sivers function [26–29].

While at the time of publication of Ref. [1] no data were available on  $A_N$  from lepton-proton inclusive processes, very recently some experimental results have been published by the HERMES Collaboration [30]. New data are also available by the JLab Hall A Collaboration [31], but their  $P_T$  values are too small (less than 0.7 GeV) to fix a large scale.

We consider here the results of the HERMES Collaboration, selecting those which best fulfil the kinematical conditions necessary for the validity of our scheme, and compare them with our calculations based on TMD factorization and the Sivers and Collins functions extracted from SIDIS data. In Sec. II we briefly summarize our formalism and in Sec. III we compare our numerical results with data and give some predictions for future measurements. Some final comments are given in Sec. IV.

## II. FORMALISM

In Ref. [1] (to which we refer for all details) we considered the process  $p^\uparrow \ell \rightarrow hX$  in the proton-lepton c.m. frame (with the polarized proton moving along the positive  $Z_{cm}$  axis) and the transverse Single Spin Asymmetry:

$$A_N = \frac{d\sigma^\uparrow(\mathbf{P}_T) - d\sigma^\downarrow(\mathbf{P}_T)}{d\sigma^\uparrow(\mathbf{P}_T) + d\sigma^\downarrow(\mathbf{P}_T)} = \frac{d\sigma^\uparrow(\mathbf{P}_T) - d\sigma^\uparrow(-\mathbf{P}_T)}{2d\sigma^{\text{unp}}(\mathbf{P}_T)}, \quad (1)$$

\*Corresponding author.  
umberto.dalesio@ca.infn.it

where

$$d\sigma^{\uparrow,\downarrow} \equiv \frac{E_h d\sigma^{p^{\uparrow,\downarrow}\ell \rightarrow hX}}{d^3\mathbf{P}_h} \quad (2)$$

is the cross section for the inclusive process  $p^{\uparrow,\downarrow}\ell \rightarrow hX$  with a transversely polarized proton with spin “up” ( $\uparrow$ ) or “down” ( $\downarrow$ ) with respect to the scattering plane [1].  $A_N$  can be measured either by looking at the production of hadrons at a fixed transverse momentum  $\mathbf{P}_T$ , changing the incoming proton polarization from  $\uparrow$  to  $\downarrow$ , or keeping a fixed proton polarization and looking at the hadron production to the left and the right of the  $Z_{cm}$  axis (see Fig. 1 of Ref. [1]).  $A_N$  was defined (and computed) for a proton in a pure spin state with a pseudovector polarization  $\mathbf{S}_T$  normal ( $N$ ) to the production plane and  $|\mathbf{S}_T| = S_T = 1$ . For a generic transverse polarization along an azimuthal direction  $\phi_S$  in the chosen reference frame, in which the  $\uparrow$  direction is given by  $\phi_S = \pi/2$ , and a polarization  $S_T \neq 1$ , one has

$$A(\phi_S, S_T) = \mathbf{S}_T \cdot (\hat{\mathbf{p}} \times \hat{\mathbf{P}}_T) A_N = S_T \sin \phi_S A_N, \quad (3)$$

where  $\mathbf{p}$  is the proton momentum. Notice that if one follows the usual definition adopted in SIDIS experiments, one simply has

$$A_{TU}^{\sin \phi_S} \equiv \frac{2}{S_T} \frac{\int d\phi_S [d\sigma(\phi_S) - d\sigma(\phi_S + \pi)] \sin \phi_S}{\int d\phi_S [d\sigma(\phi_S) + d\sigma(\phi_S + \pi)]} = A_N. \quad (4)$$

Assuming the validity of the TMD factorization scheme for the process  $p\ell \rightarrow hX$  in which the only large scale detected is the transverse momentum  $P_T$  of the final hadron in the proton-lepton c.m. frame, the main contribution to  $A_N$  comes from the Sivers and Collins effects, and one has [1,32–34]:

$$A_N = \frac{\sum_{q,\{\lambda\}} \int \frac{dx dz}{16\pi^2 x z^2 s} d^2\mathbf{k}_\perp d^3\mathbf{p}_\perp \delta(\mathbf{p}_\perp \cdot \hat{\mathbf{p}}'_q) J(p_\perp) \delta(\hat{s} + \hat{t} + \hat{u}) [\Sigma(\uparrow) - \Sigma(\downarrow)]^{q\ell \rightarrow q\ell}}{\sum_{q,\{\lambda\}} \int \frac{dx dz}{16\pi^2 x z^2 s} d^2\mathbf{k}_\perp d^3\mathbf{p}_\perp \delta(\mathbf{p}_\perp \cdot \hat{\mathbf{p}}'_q) J(p_\perp) \delta(\hat{s} + \hat{t} + \hat{u}) [\Sigma(\uparrow) + \Sigma(\downarrow)]^{q\ell \rightarrow q\ell}}, \quad (5)$$

with

$$\begin{aligned} \sum_{\{\lambda\}} [\Sigma(\uparrow) - \Sigma(\downarrow)]^{q\ell \rightarrow q\ell} &= \frac{1}{2} \Delta^N f_{q/p^\uparrow}(x, k_\perp) \cos \phi [|\hat{M}_1^0|^2 + |\hat{M}_2^0|^2] D_{h/q}(z, p_\perp) \\ &+ h_{1q}(x, k_\perp) \hat{M}_1^0 \hat{M}_2^0 \Delta^N D_{h/q^\uparrow}(z, p_\perp) \cos(\phi' + \phi_q^h) \end{aligned} \quad (6)$$

and

$$\sum_{\{\lambda\}} [\Sigma(\uparrow) + \Sigma(\downarrow)]^{q\ell \rightarrow q\ell} = f_{q/p}(x, k_\perp) [|\hat{M}_1^0|^2 + |\hat{M}_2^0|^2] D_{h/q}(z, p_\perp). \quad (7)$$

All functions and all kinematical and dynamical variables appearing in the above equations are exactly defined in Ref. [1] and its Appendixes and in Ref. [33]. We simply recall here their meaning and physical interpretation.

- (i)  $\mathbf{k}_\perp$  is the transverse momentum of the parton in the proton and  $\mathbf{p}_\perp$  is the transverse momentum of the final hadron with respect to the direction of the fragmenting parent parton, with momentum  $\mathbf{p}'_q$ .  $\phi$  is the azimuthal angle of  $\mathbf{k}_\perp$ .
- (ii) The first term on the rhs of Eq. (6) shows the contribution to  $A_N$  of the Sivers function  $\Delta^N f_{q/p^\uparrow}(x, k_\perp)$  [35–37],

$$\begin{aligned} \Delta \hat{f}_{q/p,S}(x, \mathbf{k}_\perp) &= \hat{f}_{q/p,S}(x, \mathbf{k}_\perp) - \hat{f}_{q/p,-S}(x, \mathbf{k}_\perp) \\ &\equiv \Delta^N f_{q/p^\uparrow}(x, k_\perp) \mathbf{S}_T \cdot (\hat{\mathbf{p}} \times \hat{\mathbf{k}}_\perp) \\ &= -2 \frac{k_\perp}{M} f_{1T}^{\perp q}(x, k_\perp) \mathbf{S}_T \cdot (\hat{\mathbf{p}} \times \hat{\mathbf{k}}_\perp). \end{aligned} \quad (8)$$

It couples to the unpolarized elementary interaction  $[\propto (|M_1^0|^2 + |M_2^0|^2)]$  and the unpolarized fragmentation function  $D_{h/q}(z, p_\perp)$ ; the  $\cos \phi$  factor arises from the  $\mathbf{S}_T \cdot (\hat{\mathbf{p}} \times \hat{\mathbf{k}}_\perp)$  correlation factor.

- (iii) The second term on the rhs of Eq. (6) shows the contribution to  $A_N$  of the unintegrated transversity distribution  $h_{1q}(x, k_\perp)$  coupled to the Collins function  $\Delta^N D_{h/q^\uparrow}(z, p_\perp)$  [37,38],

$$\begin{aligned} \Delta \hat{D}_{h/q^\uparrow}(z, \mathbf{p}_\perp) &= \hat{D}_{h/q^\uparrow}(z, \mathbf{p}_\perp) - \hat{D}_{h/q^\downarrow}(z, \mathbf{p}_\perp) \\ &\equiv \Delta^N D_{h/q^\uparrow}(z, p_\perp) \mathbf{s}_q \cdot (\hat{\mathbf{p}}'_q \times \hat{\mathbf{p}}_\perp) \\ &= \frac{2p_\perp}{zm_h} H_1^{\perp q}(z, p_\perp) \mathbf{s}_q \cdot (\hat{\mathbf{p}}'_q \times \hat{\mathbf{p}}_\perp). \end{aligned} \quad (9)$$

This nonperturbative effect couples to the spin transfer elementary interaction  $(d\hat{\sigma}^{q^\uparrow \ell \rightarrow q^\uparrow \ell} - d\hat{\sigma}^{q^\uparrow \ell \rightarrow q^\downarrow \ell} \propto \hat{M}_1^0 \hat{M}_2^0)$ . The factor  $\cos(\phi' + \phi_q^h)$  arises from phases

in the  $\mathbf{k}_\perp$ -dependent transversity distribution, the Collins function and the elementary polarized interaction.

Some final comments on the kinematical configuration and the notations adopted in the HERMES experiment, with respect to those of Ref. [1], are necessary. According to the usual conventions adopted for SIDIS processes, in HERMES paper [30] the lepton is assumed to move along the positive  $Z_{cm}$  axis, so that the processes we are considering here are  $\ell p^\uparrow \rightarrow hX$ , rather than  $p^\uparrow \ell \rightarrow hX$ . In this reference frame the  $\uparrow$  ( $\downarrow$ ) direction is still along the  $+Y_{cm}$  ( $-Y_{cm}$ ) axis as in Ref. [1] and, keeping the usual definition of  $x_F = 2P_L/\sqrt{s}$ , where  $P_L$  is the longitudinal momentum of the final hadron, only its sign is reversed.

The azimuthal dependent cross section measured by HERMES is defined as [30]

$$d\sigma = d\sigma_{UU}[1 + S_T A_{UT}^{\sin\psi} \sin\psi], \quad (10)$$

where

$$\sin\psi = S_T \cdot (\hat{\mathbf{P}}_T \times \hat{\mathbf{k}}) \quad (11)$$

coincides with our  $\sin\phi_S$  of Eq. (3), as  $\mathbf{p}$  and  $\mathbf{k}$  (respectively, the proton and the lepton three-momenta) are opposite vectors in the lepton-proton c.m. frame. Indeed, taking into account that “left” and “right” are interchanged in Refs. [1] and [30] (as these are defined looking downstream along opposite directions, respectively, the proton and the lepton momentum directions) and the definition of  $x_F$ , one has

$$A_{UT}^{\sin\psi}(x_F, P_T) = A_N^{p^\uparrow \ell \rightarrow hX}(-x_F, P_T), \quad (12)$$

where  $A_N^{p^\uparrow \ell \rightarrow hX}$  is the SSA as given by Eq. (5) and computed in Ref. [1], and  $A_{UT}^{\sin\psi}$  is the quantity measured by HERMES [30].

### III. ESTIMATES FOR $A_{UT}^{\sin\psi}$ , COMPARISONS WITH DATA AND PREDICTIONS

In this section we present our estimates for  $A_{UT}^{\sin\psi}$ , following the notation and convention adopted by the HERMES experiment. In our computation, based on the TMD factorization, we consider two different sets of Siverson and Collins functions (the latter coupled to the transversity distribution), as previously obtained in a series of papers from fits of SIDIS and  $e^+e^-$  data [39–42].

These sets, besides some different initial assumptions, differ in the choice of the collinear fragmentation functions (FFs). More precisely, we adopt the Siverson functions extracted in Ref. [39], where only up and down quark contributions were considered, together with the first extraction of the transversity and Collins functions obtained in Ref. [40]. In such studies we adopted, and keep using

here, the Kretzer set for the collinear FFs [43]. We shall refer to this set of functions as the SIDIS 1 set.

We then consider a more recent extraction of the Siverson functions [41], where also the sea quark contributions were included, together with an updated version of the transversity and Collins functions [42]; in these cases we adopted another set for the FFs, namely that by de Florian, Sassot and Stratmann (DSS) [44]. We shall refer to these as the SIDIS 2 set.

The use of these two sets of parametrizations, with their peculiar differences, allows to take into account both the role of different weights between leading and nonleading collinear FFs, as well as the different behavior in the large  $x$  region of the Siverson and transversity distributions. The large  $x$  behavior of these functions is still largely unconstrained by SIDIS data, while it might be relevant to explain the values of  $A_N$  measured in  $p^\uparrow p \rightarrow \pi X$  processes at RHIC, as studied in Refs. [45,46]. As this paper focuses on a process kinematically much closer to SIDIS, the large  $x$  behavior of the involved TMDs is not so relevant here. Our two sets of TMDs (SIDIS 1 and SIDIS 2) are well representative of the possible uncertainties.

We then simply compute the values of  $A_N$  as resulting, in the TMD factorized scheme, from the—SIDIS and  $e^+e^-$  extracted—SIDIS 1 and SIDIS 2 sets of TMDs. We will also show the uncertainty bands obtained by combining the statistical uncertainty bands of the Siverson and Collins functions, given by the procedure described in Appendix A of Ref. [41].

In the following we will consider both the fully inclusive data from  $\ell p \rightarrow \pi X$  processes at large  $P_T$ , as well as the subsample of data from processes in which also the final lepton is tagged (SIDIS category). In the first case there is only one large scale, the  $P_T$  of the final pion, and for  $P_T \simeq 1$  GeV, in order to avoid the low  $Q^2$  region, one has to look at pion production in the backward proton hemisphere (according to the HERMES conventions this means  $x_F > 0$ ). In this region (large  $P_T$  and  $x_F > 0$ ) the lepton-quark scattering is still dominated by  $Q^2 \geq 1$  GeV<sup>2</sup> and our pQCD computation is under control.

For the tagged-lepton subsample data  $Q^2$  is measured and chosen to be always bigger than 1 GeV<sup>2</sup>. Notice that even in such conditions, working in the lepton-proton c.m. frame,  $P_T$  is still defined as the transverse momentum of the pion with respect to the lepton-proton direction. We will refer to these data as the “SIDIS category.”

Another important aspect to keep in mind is that in both cases (inclusive or lepton-tagged events), one is not able to separate the single contributions to  $A_N$  of the Siverson and Collins effects, which in principle could contribute together.

#### A. Fully inclusive case

In this case, in order to apply our TMD factorized approach, one has to consider data at large  $P_T$ . Among the HERMES data there is one bin that fulfils this requirement,

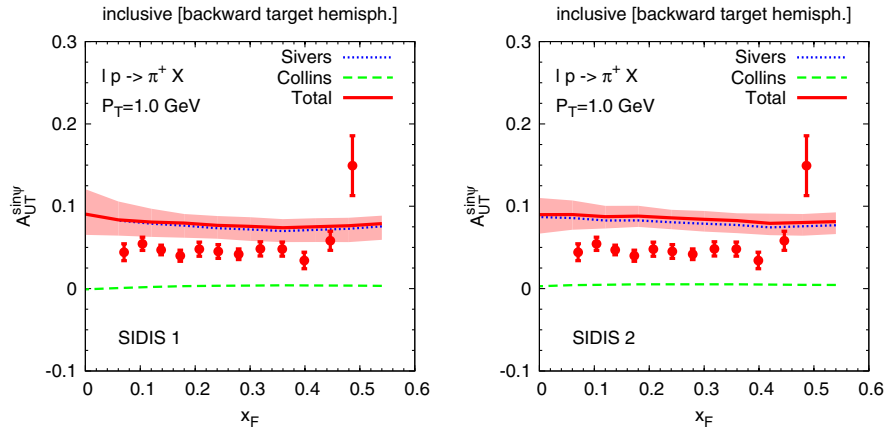


FIG. 1 (color online). The theoretical estimates for  $A_{UT}^{\sin\psi}$  vs  $x_F$  at  $\sqrt{s} \approx 7$  GeV and  $P_T = 1$  GeV for inclusive  $\pi^+$  production in  $\ell p \rightarrow \pi X$  processes, computed according to Eqs. (12) and (5)–(7) of the text, are compared with the HERMES data [30]. The contributions from the Siverson (dotted blue lines) and the Collins (dashed green lines) effects are shown separately and also added together (solid red lines). The computation is performed adopting the Siverson and Collins functions of Refs. [39,40], referred to as SIDIS 1 in the text (left panel), and of Refs. [41,42], SIDIS 2 in the text (right panel). The overall statistical uncertainty band, also shown, is the envelope of the two independent statistical uncertainty bands obtained following the procedure described in Appendix A of Ref. [41].

with  $1 \lesssim P_T \lesssim 2.2$  GeV, and  $\langle P_T \rangle \approx 1$ –1.1 GeV. In Figs. 1 and 2 we show a comparison of our estimates with these data, respectively, for positive and negative pion production. More precisely, we show the results coming from both sets of TMDs, SIDIS 1 (left panels) and SIDIS 2 (right panels), for the Siverson (dotted blue lines) and Collins (dashed green lines) effects separately, together with their sum (solid red lines). We also computed the statistical uncertainty bands for both effects and showed the envelope of the two bands (shaded area). Some comments are in order:

- (i) In this kinematical region the Collins effect is always negligible, almost compatible with zero. The reason is twofold: from one side the partonic spin transfer in the backward proton hemisphere is dynamically suppressed, as explained in Ref. [1]; secondly, the azimuthal phase [see the second term on the rhs of Eq. (6)] oscillates strongly, washing out the effect.
- (ii) The Siverson effect does not suffer from any dynamical suppression, since it enters with the unpolarized partonic cross section. Moreover, there is no suppression from the integration over the azimuthal phases, as it happens, for instance, in  $pp \rightarrow \pi X$  case. Indeed in  $\ell p \rightarrow \pi X$  only one partonic channel is at work and, for the moderate  $Q^2$  values of HERMES kinematics, the Siverson phase ( $\phi$ ) appearing in the first term on the rhs of Eq. (6) appears also significantly in the elementary interaction, thus resulting in a nonzero phase integration.
- (iii) Moreover, in this kinematical region, even if looking at the backward hemisphere of the polarized proton, one probes its valence region, where the extracted Siverson functions are well constrained. The reason is basically related to the moderate c.m. energy,  $\sqrt{s} \approx 7$  GeV, of the HERMES experiment.

- (iv) The difference between SIDIS 1 and SIDIS 2 results for the negative pion case, Fig. 2, comes from the fact that in the first case the Siverson function for up quark plays a relative bigger role, even if coupled with the nonleading FF.
- (v) The results presented here for the SIDIS 2 set of TMDs correspond to the predictions given in Ref. [1], with the difference that they were obtained for  $P_T = 1.5$  and 2.5 GeV, and one should change  $x_F$  into  $-x_F$ .
- (vi) Quasireal photoproduction of large transverse momentum hadrons could in principle give a substantial contribution to the cross section. As mentioned in the previous section, in order to minimize this contribution we have considered only large  $P_T$  and large positive  $x_F$  (backward proton hemisphere) values. In this kinematical regions  $Q^2$  is predominantly larger than 1 GeV<sup>2</sup>. It will be very interesting to compare our predictions to a direct measurement of the cross sections along with the asymmetries.

As one can see, while the SSA for positive pion production is a bit overestimated, Fig. 1, the description of the negative pion SSAs is in fair agreement with data for the SIDIS 1 set (left panel in Fig. 2). Notice that in the fully inclusive case under study, at such values of  $\sqrt{s}$  and  $Q^2$  other effects could contaminate the SSA. Nonetheless the qualitative description, in size, shape and sign, is quite encouraging.

## B. Tagged or semi-inclusive category

The HERMES Collaboration presents also a subsample of  $\ell p$  data where the final lepton is tagged [30]. Of course the number of these events is strongly reduced with respect to the fully inclusive case. Nonetheless the observed asymmetries are sizeable and show a peculiar behavior.

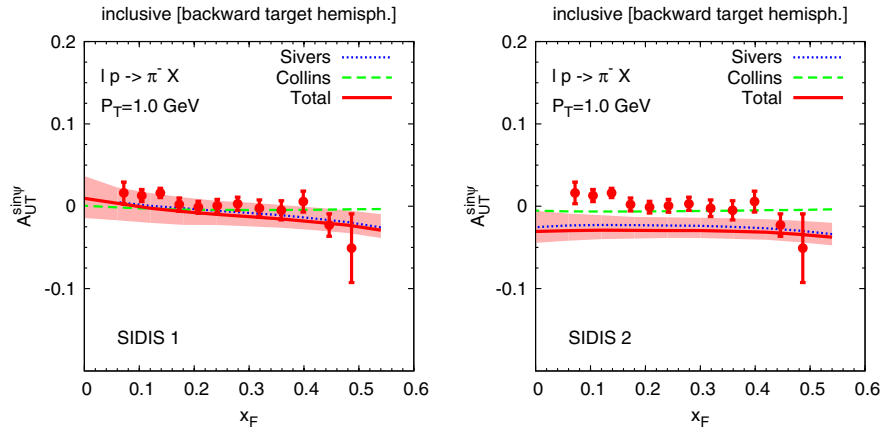


FIG. 2 (color online). Same as in Fig. 1 but for inclusive  $\pi^-$  production.

We then consider also these data by imposing HERMES cuts:  $Q^2 > 1 \text{ GeV}^2$ ,  $W^2 > 10 \text{ GeV}^2$ ,  $0.023 < x_B < 0.4$ ,  $0.1 < y < 0.95$  and  $0.2 < z_h < 0.7$ , where these are the standard variables adopted for the study of SIDIS processes. Even in this case we restrict the analysis to the large  $P_T$  region, namely  $P_T > 1 \text{ GeV}$ . In fact, in contrast to the SIDIS azimuthal asymmetries analyzed in the  $\gamma^* - p$  c.m. frame, where the low  $P_T \leq 1 \text{ GeV}$  of the final hadron is entirely given at leading order in terms of the intrinsic transverse momenta in the distribution and fragmentation functions, here, working in the  $\ell - p$  c.m. frame, the observed  $P_T$  is also given by the hard scattering process. For this reason, to be sensitive to the intrinsic transverse momentum effects, one has not to consider necessarily very small  $P_T$  values.

We show our estimates compared with HERMES data in Figs. 3 and 4, respectively, for positive and negative pion production as a function of  $P_T$  at fixed  $x_F = 0.2$ . Notice that for  $P_T > 1 \text{ GeV}$ , the values of  $x_F$  probed in the HERMES kinematics are all very close to 0.2. We checked that increasing the value of  $x_F$ , up to 0.3, the results are

almost unchanged. Again, we show the contributions from the Siverson (dotted blue line) and Collins (dashed green line) effects separately and added together (solid red line) with the overall uncertainty bands (shaded area). Some comments follow:

- (i) In this region the Collins effect (dashed green lines) is only partially suppressed by the dynamics and the azimuthal phase integration. Indeed the spin transfer is still sizeable and the azimuthal phase entering the Collins effect is peaked around  $\pi$ , that is the  $\cos(\phi' + \phi_q^h)$  in the second term on the rhs of Eq. (6) is peaked around  $-1$ . Keeping in mind that the partonic spin transfer is always positive and that the convolution of the transversity distributions with the Collins functions is positive for  $\pi^+$  and negative for  $\pi^-$ , one can understand the sign of this contribution. The difference between the SIDIS 1 and the SIDIS 2 sets (a factor around 2–3) comes from the different behavior of the quark transversity functions at moderately large  $x$ .

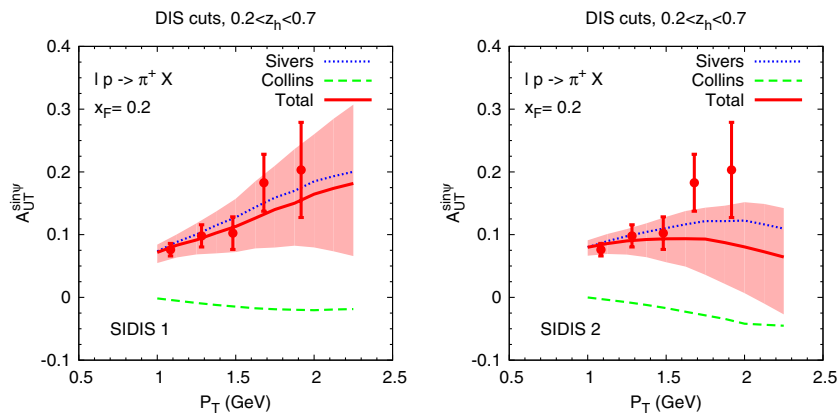
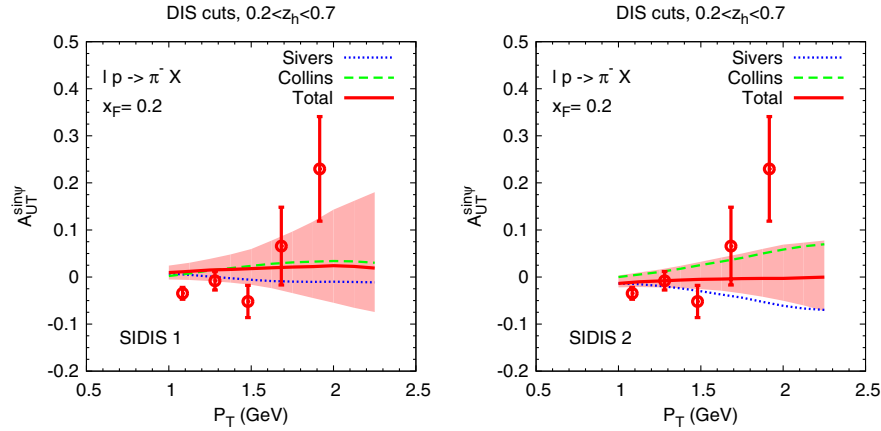


FIG. 3 (color online). The theoretical estimates for  $A_{UT}^{\sin\psi}$  vs  $P_T$  at  $\sqrt{s} \approx 7 \text{ GeV}$  and  $x_F = 0.2$  for inclusive  $\pi^+$  production for the lepton tagged events in  $\ell p \rightarrow \pi X$  process, computed according to Eqs. (12) and (5)–(7) of the text, are compared with the HERMES data [30]. The contributions from the Siverson (dotted blue lines) and the Collins (dashed green lines) effects are shown separately and also added together (solid red lines). The computation is performed adopting the Siverson and Collins functions of Refs. [39,40], referred as SIDIS 1 in the text (left panel), and of Refs. [41,42], SIDIS 2 in the text (right panel). The overall statistical uncertainty band, also shown, is the envelope of the two independent statistical uncertainty bands obtained following the procedure described in Appendix A of Ref. [41].


FIG. 4 (color online). Same as in Fig. 3 but for  $\pi^-$  production.

- (ii) The Siverson effect (dotted blue lines) for  $\pi^+$  production (Fig. 3) is sizeable for both sets. On the other hand for  $\pi^-$  production (Fig. 4) the SIDIS 1 set (left panel) gives almost zero due to the strong cancellation between the unsuppressed Siverson up quark distribution coupled to the nonleading FF, with the more suppressed down quark distribution. In the SIDIS 2 set (right panel), the same large  $x$  behavior of the up and down quark Siverson distributions implies no cancellation.
- (iii) With the exception of the largest  $P_T$  data point the description of the data in terms of the sum of these effects is fairly good for both sets.

### C. Predictions

Data at  $P_T \approx 1$  GeV are expected from the future JLab 12 operation at 11 GeV. Because of the rather low c.m. energy ( $\sqrt{s} \approx 4.8$  GeV), in order to select data with large values of  $Q^2$  one has to consider a backward (with respect

to the proton direction) production, which means  $x_F \geq 0.1$ . With these kinematical bounds most contribution come from the quark valence region. Our predictions, analogous to the results presented in Figs. 1 and 2, are shown in Figs. 5 and 6. The results expected at JLab 12 are similar to those observed at HERMES.

One might also wonder whether some features that characterize the SSAs observed in  $pp \rightarrow \pi X$  processes and that can be reproduced within a TMD factorization scheme [45], could still be encountered in  $\ell p \rightarrow \pi X$  reactions. To answer this question we consider the inclusive  $\ell p$  process at  $\sqrt{s} = 50$  GeV. In this case, in order to have a more direct comparison with the  $p^\uparrow p$  case, we calculate  $A_N$  as defined in Eq. (6), with the polarized proton moving along  $Z_{cm}$ , that is with positive  $x_F$  in the forward hemisphere of the polarized proton. In Fig. 7 we show our estimates of  $A_N$  for  $\pi^0$  production in the process  $p^\uparrow \ell \rightarrow \pi X$  at  $\sqrt{s} = 50$  GeV and  $P_T = 1$  GeV (left panel) and  $P_T = 2$  GeV (right panel) adopting the SIDIS 1 set. This set

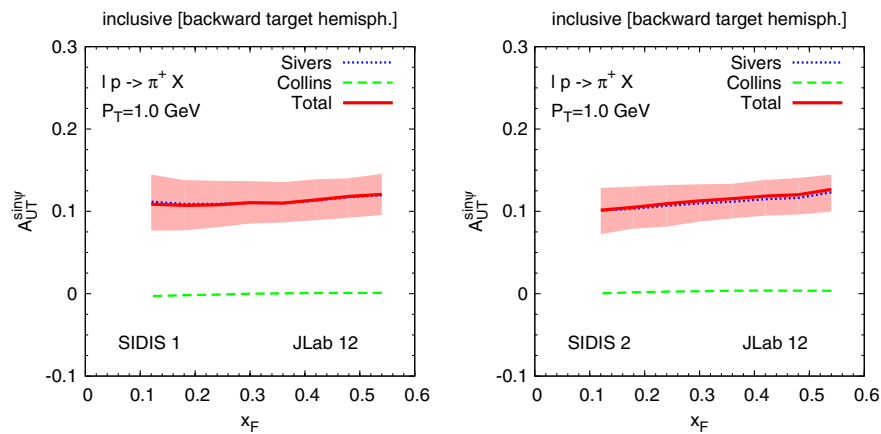


FIG. 5 (color online). Theoretical predictions for  $A_{UT}^{\sin\psi}$  vs  $x_F$  at  $\sqrt{s} \approx 4.8$  GeV and  $P_T = 1$  GeV for inclusive  $\pi^+$  production in  $\ell p^\uparrow \rightarrow \pi X$  processes, computed according to Eqs. (12) and (5)–(7) of the text, are shown for future JLab experiments. The contributions from the Siverson (dotted blue lines) and the Collins (dashed green lines) effects are shown separately and also added together (solid red lines). The computation is performed adopting the Siverson and Collins functions of Refs. [39,40], referred to as SIDIS 1 in the text (left panel), and of Refs. [41,42], SIDIS 2 in the text (right panel). The overall statistical uncertainty band, also shown, is the envelope of the two independent statistical uncertainty bands obtained following the procedure described in Appendix A of Ref. [41].

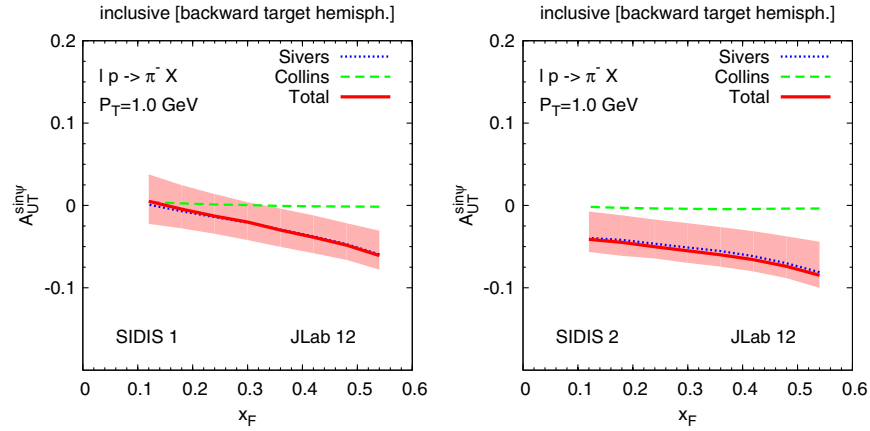


FIG. 6 (color online). Same as in Fig. 5 but for inclusive  $\pi^-$  production.

indeed is the one that better reproduces the behavior of  $A_N$  in  $p^\uparrow p \rightarrow \pi X$  processes (see for instance Ref. [47]). The result deserves a few comments.

- (i) The Collins effect in the backward region is totally negligible: this is due to a strong suppression coming from the azimuthal phase integration. In the forward region the SIDIS 1 set, as well the SIDIS 2 (results not shown), give tiny values even if the azimuthal phase would be effective. In particular for  $x_F > 0.3$ , once again the cosine factor entering this effect in Eq. (6) is negative.
- (ii) The Siverts effect is sizeable and increasing with  $x_F$  for positive values of  $x_F$ , while negligible in the negative  $x_F$  region. Notice that the suppression of the Siverts effect for  $x_F < 0$ , even if in such a process there is only one partonic channel, is due to a weak dependence on the azimuthal phase of the elementary interaction at the large  $Q^2$  values reached at these energies.
- (iii) It is worth noticing that the functional shape of  $A_N(x_F)$ , for the  $p^\uparrow \ell \rightarrow hX$  large  $P_T$  process, is

similar to that observed at various energies in  $p^\uparrow p \rightarrow hX$  processes, being negligible at negative  $x_F$  and increasing with positive values of  $x_F$ .

- (iv) The process  $\ell p^\uparrow \rightarrow \text{jet} + X$  at large  $\sqrt{s}$  values was studied in a twist-three formalism in Ref. [25]. The quark-gluon-quark Qiu-Sterman correlator  $T_F$  was fixed exploiting its relation with the Siverts function, taken from an extraction [41] from SIDIS data. The value of  $A_N$  was found to be positive for  $x_F > 0$  (the same kinematical configuration as for our Fig. 7 was adopted), with results very close to the results we find here for  $\pi^0$  production and we found in Ref. [1] for jet production. Indeed the twist-three and the TMD mechanisms were shown to be closely related and provide a unified picture for SSAs in SIDIS processes [48]. However, the factorized twist-three collinear scheme, using the SIDIS extracted Siverts functions for fixing the Qiu-Sterman correlator  $T_F$ , seems to have severe problems in explaining the SSA  $A_N$  observed in  $pp$  processes, leading to values

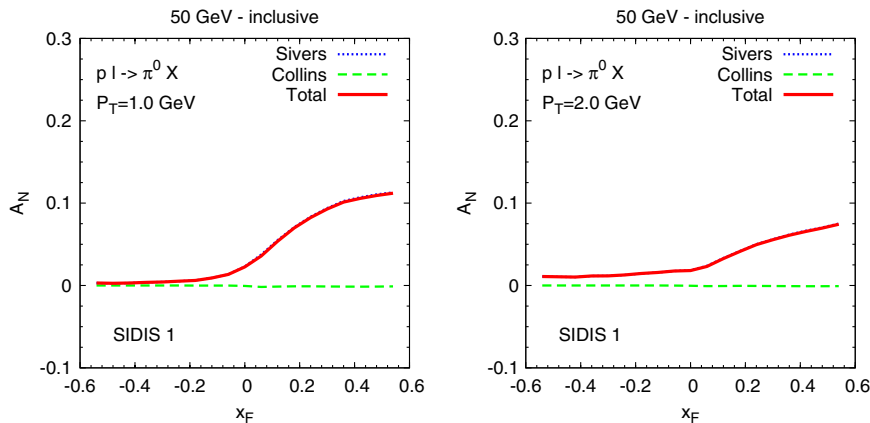


FIG. 7 (color online). Theoretical estimates of  $A_N$  vs  $x_F$  at  $\sqrt{s} \approx 50$  GeV,  $P_T = 1$  GeV (left panel) and  $P_T = 2$  GeV (right panel) for inclusive  $\pi^0$  production in the  $p^\uparrow \ell \rightarrow \pi X$  process. Notice that, contrary to the kinematical configurations of Figs. 1 and 2, a forward production with respect to the proton direction corresponds here to positive values of  $x_F$ . The contributions from the Siverts (dotted blue lines) and the Collins (dashed green lines) effects are shown separately and also added together (solid red lines). The estimates are obtained adopting the Siverts and Collins functions of Refs. [39,40] (SIDIS 1 set), according to Eqs. (5)–(7) of the text.

of  $A_N$  opposite to those measured [49]. These issues were further studied in Refs. [50–52]. A recent analysis of  $A_N$  in  $pp$  scattering in the twist-three formalism [53] attempts at solving this problem showing that the asymmetry might be dominated by new large effects coming from fragmentation. It is not clear how much these same effects would change the value of  $A_N$  in SIDIS when going from jet to  $\pi^0$  production.

- (v) The measurement of asymmetries in the same kinematical region and with the same features as in Fig. 7 for  $\pi^0$  production, and as in Fig. 6 of Ref. [1] for jet production, would be a strong indication in support of our TMD factorized approach. Such measurements might be possible at a future electron-ion collider (EIC) [54].

#### IV. COMMENTS AND CONCLUSIONS

We have further pursued and tested the idea presented in Ref. [1] for assessing the validity of the TMD factorization in inclusive processes in which a single large  $P_T$  particle is produced. Starting from the TMD factorization valid for SIDIS processes,  $\ell p \rightarrow \ell hX$ , in which a large  $Q^2$  virtual photon  $\gamma^*$  hits a quark, which then fragments into a final hadron with a small  $P_T$  in the  $\gamma^* - p$  c.m. frame, we have assumed its validity for processes in which the final lepton is not necessarily observed, but the final detected hadron has a large  $P_T$  in the lepton-proton c.m. frame. A large value of  $P_T$  implies, at leading order, a large angle elementary scattering,  $\ell q \rightarrow \ell q$ , and then a large value of  $Q^2$ . Such a process is analogous to the  $p^\uparrow p \rightarrow hX$  processes, for which large SSAs  $A_N$ , Eq. (1), have been measured. According to the TMD factorization approach, the SSAs can be generated by the Siverson and Collins effects [45,46].

We have computed the single spin asymmetry  $A_N$ , for the  $\ell p^\uparrow \rightarrow hX$  process and in the TMD factorized scheme, as generated by the Siverson and the Collins functions, which have been extracted from SIDIS and  $e^+e^-$  data [39–42]. Doing so, we adopt a unified TMD factorized approach, valid for  $\ell p \rightarrow \ell hX$  and  $\ell p \rightarrow hX$  processes, in which, consistently, we obtain information on the TMDs and make predictions for  $A_N$ . Some of these predictions were given in Ref. [1].

New HERMES data on  $A_N$  are now available [30] for different kinematical regions; we have selected those data which—although not yet optimally—fulfil the conditions of applicability of our TMD factorization approach, and compared them with the results of our computations. We have selected two sets of TMDs extracted from SIDIS and  $e^+e^-$  data, and which are representative, with their large differences, of the uncertainties which the SIDIS available data still allow.

It turns out, Figs. 1, 2, 3, and 4, that our theoretical estimates for  $A_{UT}^{\sin\psi}(x_F, P_T) = A_N(-x_F, P_T)$  agree well, in shape and sign, with the experimental results, in particular for one set of TMDs (SIDIS 1). In some cases (see Fig. 1) our results are a bit larger than data, yet with the right sign and behavior; one should not forget that in the kinematical regions we are considering (in  $P_T$ ,  $Q^2$  and  $\sqrt{s}$ ) other mechanisms might still be at work. The overall agreement between our computations and the data is very encouraging.

In Figs. 5 and 6 we have estimated the expected value of  $A_{UT}^{\sin\psi}$  at the future JLab experiments at 12 GeV. We are still in a kinematical region where a careful selection of data is necessary in order to ensure the validity of our approach. The results are similar to those obtained in Figs. 1 and 2 for HERMES kinematics.

At last, in Fig. 7, we have given predictions for  $A_N(x_F)$  in very safe kinematical regions for our approach to hold. Indeed, as expected, we recover the same behavior for  $A_N(x_F)$  as observed in  $p^\uparrow p \rightarrow \pi^0 X$  processes. Such a prediction, crucial for assessing the validity of our TMD factorization scheme, could be tested at a future EIC [54].

#### ACKNOWLEDGMENTS

A.P. work is supported by the U.S. Department of Energy under Contract No. DE-AC05-06OR23177. M. A., M. B., U. D., S. M. and F. M. acknowledge support from the European Community under the FP7 program “Capacities—Research Infrastructures” (HadronPhysics3, Grant Agreement No. 283286). M. A., M. B. and S. M. acknowledge support from the “Progetto di Ricerca Ateneo/CSP” (codice TO-Call3-2012-0103). U. D. is grateful to the Department of Theoretical Physics II of the Universidad Complutense of Madrid for the kind hospitality extended to him during the completion of this work.

[1] M. Anselmino, M. Boglione, U. D’Alesio, S. Melis, F. Murgia, and A. Prokudin, *Phys. Rev. D* **81**, 034007 (2010).  
 [2] D. L. Adams *et al.* (E581 Collaboration and E704 Collaboration), *Phys. Lett. B* **261**, 201 (1991).

[3] D. L. Adams *et al.* (E704 Collaboration), *Phys. Lett. B* **264**, 462 (1991).  
 [4] D. L. Adams *et al.* (E581 Collaboration and E704 Collaboration), *Phys. Lett. B* **276**, 531 (1992).



- [5] D. L. Adams *et al.* (E581 Collaboration), *Z. Phys. C* **56**, 181 (1992).
- [6] J. Adams *et al.* (STAR Collaboration), *Phys. Rev. Lett.* **92**, 171801 (2004).
- [7] S. S. Adler *et al.* (PHENIX Collaboration), *Phys. Rev. Lett.* **95**, 202001 (2005).
- [8] J. H. Lee and F. Videbaek (BRAHMS Collaboration), *AIP Conf. Proc.* **915**, 533 (2007).
- [9] B. Abelev *et al.* (STAR Collaboration), *Phys. Rev. Lett.* **101**, 222001 (2008).
- [10] L. Adamczyk *et al.* (STAR Collaboration), *Phys. Rev. D* **86**, 051101 (2012).
- [11] G. Igo *et al.* (STAR Collaboration), *AIP Conf. Proc.* **1523**, 188 (2013).
- [12] L. C. Bland *et al.* (AnDY Collaboration), [arXiv:1304.1454](https://arxiv.org/abs/1304.1454).
- [13] J. C. Collins, *Phys. Lett. B* **536**, 43 (2002).
- [14] J. C. Collins and A. Metz, *Phys. Rev. Lett.* **93**, 252001 (2004).
- [15] X.-d. Ji, J.-p. Ma, and F. Yuan, *Phys. Rev. D* **71**, 034005 (2005).
- [16] X.-d. Ji, J.-p. Ma, and F. Yuan, *Phys. Lett. B* **597**, 299 (2004).
- [17] A. Bacchetta, D. Boer, M. Diehl, and P. J. Mulders, *J. High Energy Phys.* **08** (2008) 023.
- [18] J. Collins, *Foundations of Perturbative QCD*, Vol. 32, Cambridge Monographs on Particle Physics, Nuclear Physics and Cosmology (Cambridge University Press, Cambridge, England, 2011).
- [19] M. G. Echevarría, A. Idilbi, and I. Scimemi, *J. High Energy Phys.* **07** (2012) 002.
- [20] M. G. Echevarría, A. Idilbi, and I. Scimemi, [arXiv:1402.0869](https://arxiv.org/abs/1402.0869).
- [21] J. She, Y. Mao, and B.-Q. Ma, *Phys. Lett. B* **666**, 355 (2008).
- [22] M. Anselmino, M. Boglione, J. Hansson, and F. Murgia, *Eur. Phys. J. C* **13**, 519 (2000).
- [23] Y. Koike, *AIP Conf. Proc.* **675**, 449 (2003).
- [24] Y. Koike, *Nucl. Phys. A* **721**, C364 (2003).
- [25] Z.-B. Kang, A. Metz, J.-W. Qiu, and J. Zhou, *Phys. Rev. D* **84**, 034046 (2011).
- [26] D. Boer, P. J. Mulders, and F. Pijlman, *Nucl. Phys. B* **667**, 201 (2003).
- [27] J. Ma and Q. Wang, *Eur. Phys. J. C* **37**, 293 (2004).
- [28] J. Zhou, F. Yuan, and Z.-T. Liang, *Phys. Rev. D* **79**, 114022 (2009).
- [29] J. Zhou, F. Yuan, and Z.-T. Liang, *Phys. Rev. D* **81**, 054008 (2010).
- [30] A. Airapetian *et al.* (HERMES Collaboration), *Phys. Lett. B* **728**, 183 (2014).
- [31] K. Allada *et al.* (Jefferson Lab Hall A Collaboration), *Phys. Rev. C* **89**, 042201 (2014).
- [32] U. D'Alesio and F. Murgia, *Phys. Rev. D* **70**, 074009 (2004).
- [33] M. Anselmino, M. Boglione, U. D'Alesio, E. Leader, S. Melis, and F. Murgia, *Phys. Rev. D* **73**, 014020 (2006).
- [34] U. D'Alesio and F. Murgia, *Prog. Part. Nucl. Phys.* **61**, 394 (2008).
- [35] D. W. Sivers, *Phys. Rev. D* **41**, 83 (1990).
- [36] D. W. Sivers, *Phys. Rev. D* **43**, 261 (1991).
- [37] A. Bacchetta, U. D'Alesio, M. Diehl, and C. A. Miller, *Phys. Rev. D* **70**, 117504 (2004).
- [38] J. C. Collins, *Nucl. Phys. B* **396**, 161 (1993).
- [39] M. Anselmino, M. Boglione, U. D'Alesio, A. Kotzinian, F. Murgia, and A. Prokudin, *Phys. Rev. D* **72**, 094007 (2005).
- [40] M. Anselmino, M. Boglione, U. D'Alesio, A. Kotzinian, F. Murgia, A. Prokudin, and C. Türk, *Phys. Rev. D* **75**, 054032 (2007).
- [41] M. Anselmino, M. Boglione, U. D'Alesio, A. Kotzinian, S. Melis, F. Murgia, A. Prokudin, and C. Türk, *Eur. Phys. J. A* **39**, 89 (2009).
- [42] M. Anselmino, M. Boglione, U. D'Alesio, A. Kotzinian, F. Murgia, A. Prokudin, and S. Melis, *Nucl. Phys. B, Proc. Suppl.* **191**, 98 (2009).
- [43] S. Kretzer, *Phys. Rev. D* **62**, 054001 (2000).
- [44] D. de Florian, R. Sassot, and M. Stratmann, *Phys. Rev. D* **75**, 114010 (2007).
- [45] M. Anselmino, M. Boglione, U. D'Alesio, S. Melis, F. Murgia, and A. Prokudin, *Phys. Rev. D* **88**, 054023 (2013).
- [46] M. Anselmino, M. Boglione, U. D'Alesio, E. Leader, S. Melis, F. Murgia, and A. Prokudin, *Phys. Rev. D* **86**, 074032 (2012).
- [47] M. Boglione, U. D'Alesio, and F. Murgia, *Phys. Rev. D* **77**, 051502 (2008).
- [48] X. Ji, J.-W. Qiu, W. Vogelsang, and F. Yuan, *Phys. Rev. Lett.* **97**, 082002 (2006).
- [49] Z.-B. Kang, J.-W. Qiu, W. Vogelsang, and F. Yuan, *Phys. Rev. D* **83**, 094001 (2011).
- [50] Z.-B. Kang and A. Prokudin, *Phys. Rev. D* **85**, 074008 (2012).
- [51] A. Metz, D. Pitonyak, A. Schafer, M. Schlegel, W. Vogelsang, and J. Zhou, *Phys. Rev. D* **86**, 094039 (2012).
- [52] L. Gamberg, Z.-B. Kang, and A. Prokudin, *Phys. Rev. Lett.* **110**, 232301 (2013).
- [53] K. Kanazawa, Y. Koike, A. Metz, and D. Pitonyak, *Phys. Rev. D* **89**, 111501(R) (2014).
- [54] A. Accardi *et al.*, [arXiv:1212.1701](https://arxiv.org/abs/1212.1701).